Insights into the effect of regulation in molecular composition on the properties of $(AuAg)_9$ clusters

Xiaoxun Yan,‡ Shangyu Su,‡ Xiaowu Li, Shan Jin,* Manzhou Zhu*

Institutes of Physical Science and Information Technology and Centre for Atomic Engineering of Advanced Materials, Key Laboratory of Structure and Functional Regulation of Hybrid Materials of Ministry of Education, Department of Chemistry and Anhui Province Key Laboratory of Chemistry for Inorganic/Organic Hybrid Functionalized Materials, Anhui University, Hefei, Anhui 230601, China

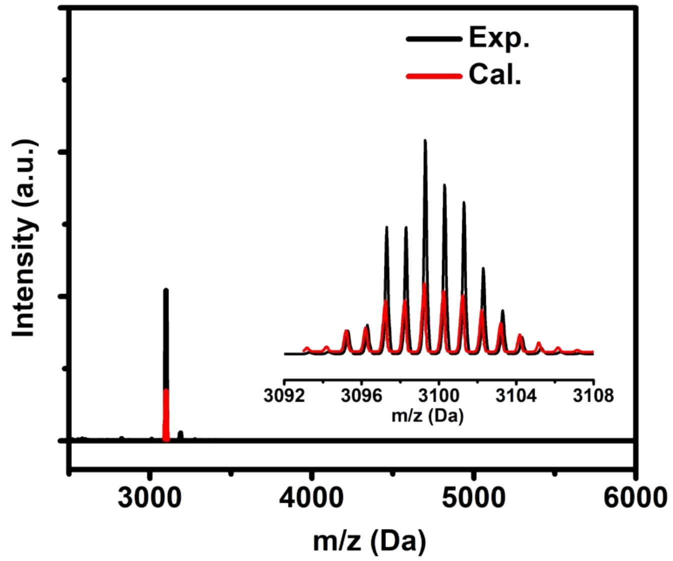

Figure S1. The ESI-MS data of $[Au_4Ag_5(SAdm)_6(Dppm)_2](BPh_4)$.

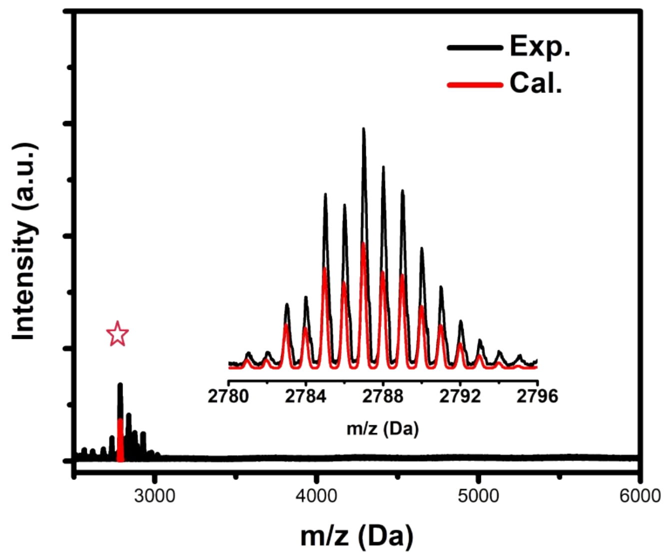

Figure S2. The ESI-MS data of $[Au_4Ag_5(S\text{-}c\text{-}C_6H_{11})_6(Dppm)_2](BPh_4)$.

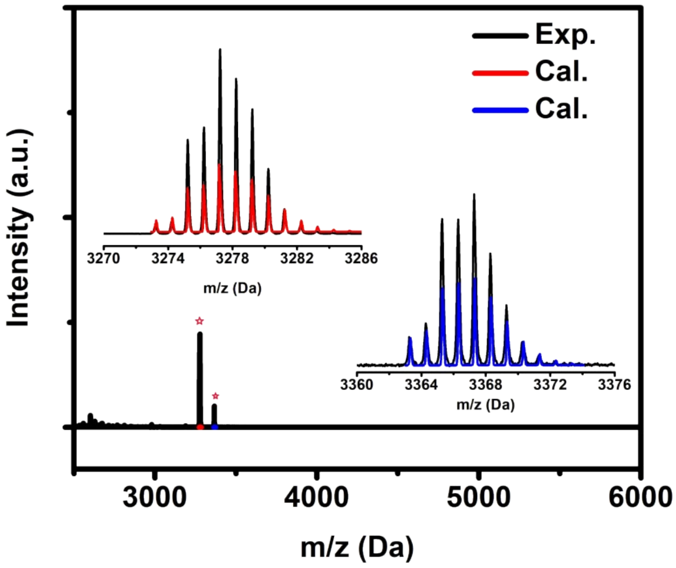

Figure S3. The ESI-MS data of $[Au_{6.5}Ag_{2.5}(SAdm)_6(Dppm)_2](BPh_4)$.

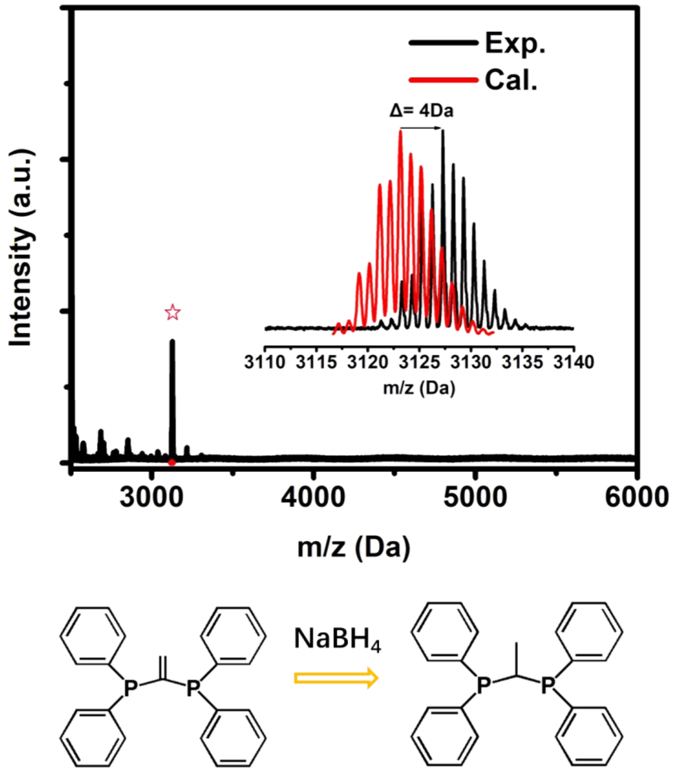

Figure S4. The ESI-MS data of $[Au_4Ag_5(SAdm)_6(VDPP)_2](BPh_4)$. The result indicatedthe $(Ph_2P)_2C{=}CH_2$ ligands are reduced to $(Ph_2P)_2CH\text{-}CH_3$ with a deviation of 2 Da for each phosphine ligand.

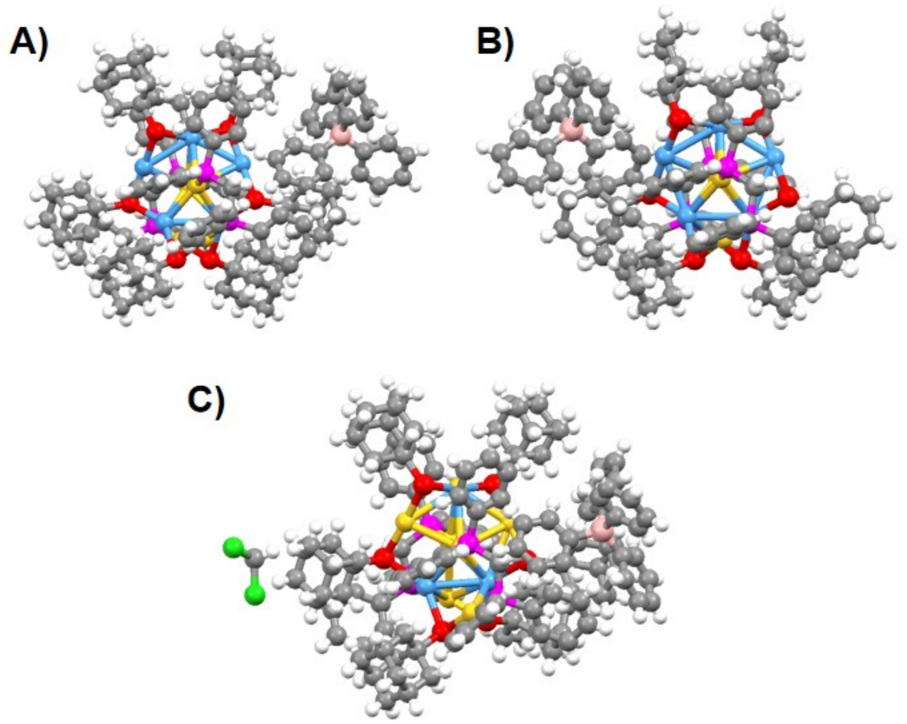

Figure S5. The overall structure of these nanoclusters. A) $[Au_4Ag_5(SAdm)_6(Dppm)_2](BPh_4)$; B) $[Au_4Ag_5(S\text{-}c\text{-}C_6H_{11})_6(Dppm)_2](BPh_4)$; C) $[Au_{6.5}Ag_{2.5}(SAdm)_6(Dppm)_2](BPh_4)$.

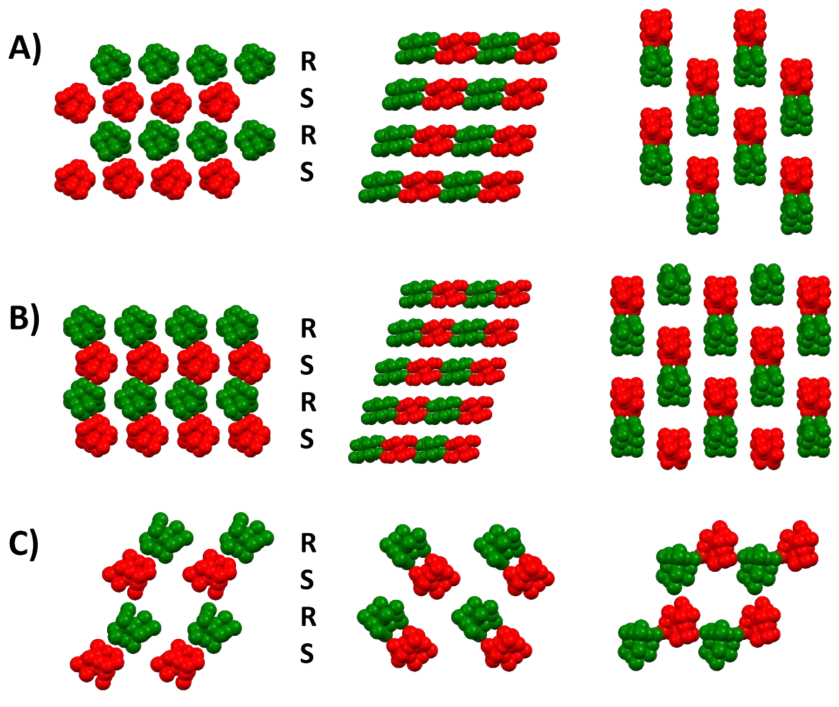

Figure S6. The the packing mode of these nanoclusters. A) $[Au_4Ag_5(SAdm)_6(Dppm)_2](BPh_4)$; B) $[Au_4Ag_5(S\text{-}c\text{-}C_6H_{11})_6(Dppm)_2](BPh_4)$; C) $[Au_{6.5}Ag_{2.5}(SAdm)_6(Dppm)_2](BPh_4)$.

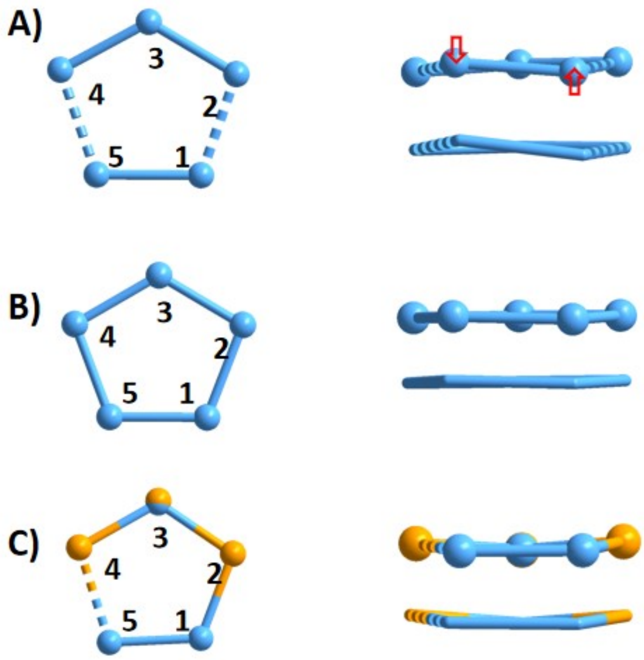

Figure S7. The framework of M_5 ring in these nanoclusters. A) $[Au_4Ag_5(SAdm)_6(Dppm)_2](BPh_4)$; B) $[Au_4Ag_5(S\text{-}c\text{-}C_6H_{11})_6(Dppm)_2](BPh_4)$; C) $[Au_{6.5}Ag_{2.5}(SAdm)_6(Dppm)_2](BPh_4)$.

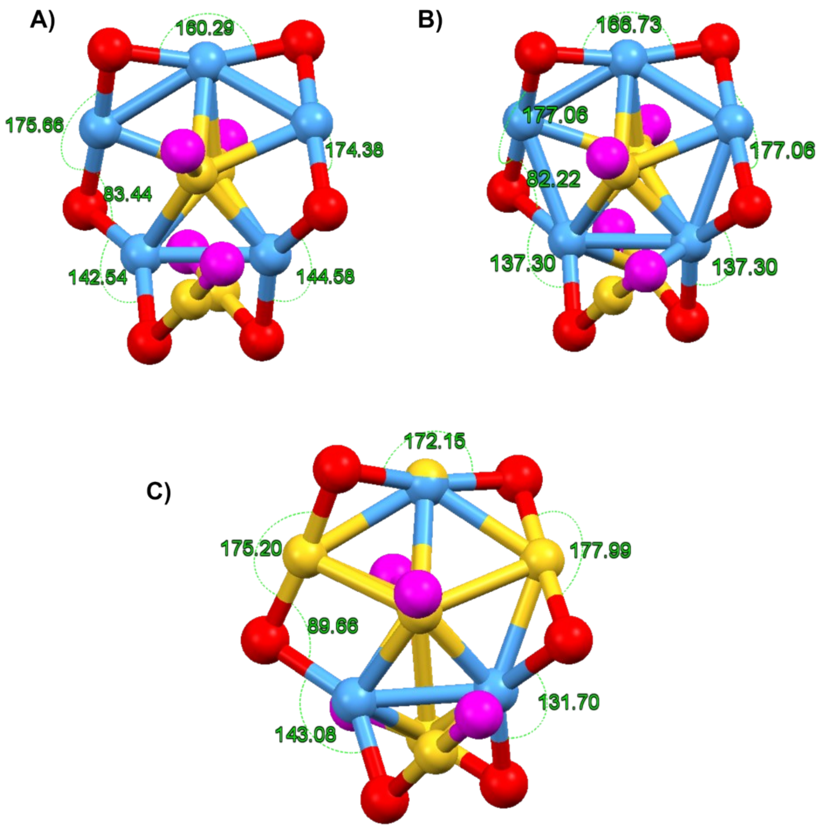

Figure S8. Different bond angles for these nanoclusters. A) $[Au_4Ag_5(SAdm)_6(Dppm)_2](BPh_4)$; B) $[Au_4Ag_5(S\text{-}c\text{-}C_6H_{11})_6(Dppm)_2](BPh_4)$; C) $[Au_{6.5}Ag_{2.5}(SAdm)_6(Dppm)_2](BPh_4)$.

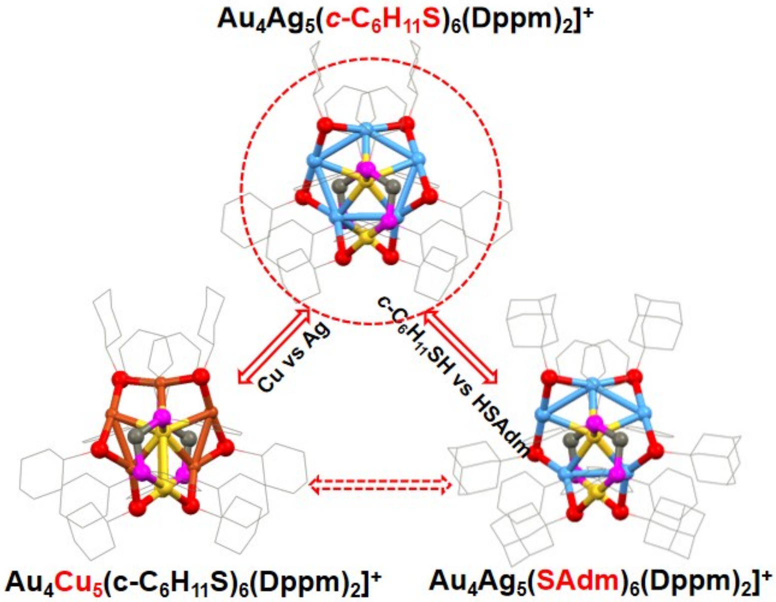

Figure S9. The obtained $[Au_4Ag_5(S\text{-}c\text{-}C_6H_{11})_6(Dppm)_2](BPh_4)$ connecting the $[Au_4Ag_5(SAdm)_6(Dppm)_2](BPh_4)$ and $[Au_4Cu_5(S\text{-}c\text{-}C_6H_{11})_6(Dppm)_2](BPh_4)$.

Table S1. Crystal data and structure refinement for Au_4Ag_5-CHT-revised.

Empirical formula	$C_{110}H_{130}Ag_5Au_4BP_4S_6$
Formula weight	3106.40
Temperature/K	120
Crystal system	monoclinic
Space group	C2/c
a/Å	24.443(3)
b/Å	25.297(3)
c/Å	18.903(3)
α/°	90
β/°	108.051(10)
γ/°	90
Volume/Å^3	11113(3)
Z	4
Radiation	CuKα (λ = 1.54186)
Index ranges	$-29 \le h \le 18$, $-30 \le k \le 28$, $-15 \le l \le 22$
Independent reflections	10308 [R_{int} = 0.0768, R_{sigma} = 0.0495]
Data/restraints/parameters	10308/1499/515
Goodness-of-fit on F^2	1.060
Final R indexes [I>=2σ (I)]	R_1 = 0.0650, wR_2 = 0.1832
Final R indexes [all data]	R_1 = 0.0744, wR_2 = 0.1916
Largest diff. peak/hole / e Å$^-$	2.02/-3.64

Table S2. Crystal data and structure refinement for $Ag_{2.48}Au_{6.53}$.

Empirical formula	$C_{134.5}H_{154}Ag_{2.48}Au_{6.53}BClP_4S_6$
Formula weight	3685.25
Temperature/K	120
Crystal system	triclinic
Space group	P-1
a/Å	18.3755(10)
b/Å	19.6063(11)
c/Å	21.8061(12)
α/°	103.741(4)
β/°	100.027(4)
γ/°	112.795(4)
Volume/Å^3	6717.4(7)
Z	2
Radiation	CuKα (λ = 1.54186)
Index ranges	$-18 \leq h \leq 22$, $-22 \leq k \leq 23$, $-26 \leq l \leq 11$
Independent reflections	23983 [R_{int} = 0.0693, R_{sigma} = 0.0731]
Data/restraints/parameters	23983/4500/1364
Goodness-of-fit on F^2	1.045
Final R indexes [I>=2σ (I)]	R_1 = 0.0906, wR_2 = 0.2447
Final R indexes [all data]	R_1 = 0.1070, wR_2 = 0.2632
Largest diff. peak/hole / e Å^{-3}	3.46/-6.45